Jour. Petrol. Soc. Korea
Vol. 3, No. 1, p. 76~93, 1994

Petrogenesis of the Precambrian Hongjesa granite
(Magmatism and metamorphism of the Proterozoic in the northeastern part of Korea)

Jeongmin Kim and Moonsup Cho

Department of Geological Sciences, Seoul National University, Seoul, 151-742 Korea

ABSTRACT : The Precambrian Hongjesa granite is lithologically zoned from biotite granite in central part to biotite-muscovite granite towards the margin. The X_{Fe} (=Fe/(Fe+Mg)) value and the aluminum saturation index of biotite systematically vary as a function of mineral assemblage, and are positively related with those of bulk rock. This relationship as well as the lithological zoning are attributed to the fractional crystallization of the Hongjesa granitic magma. The trace element data corroborate that biotite-muscovite granite is more fractionated than biotite granite. The evolution of the Hongjesa granite is elucidated by using the AFM liquidus topology, where $A=Al_2O_3-CaO-Na_2O-K_2O$; $F=FeO+MnO$; and $M=MgO$. At an early magmatic stage where biotite is the only ferromagnesian mineral to crystallize, the X_{Fe} value and the alumina content of granitic magma continuously increase. Muscovite subsequently crystallizes with biotite along the biotite-muscovite cotectic curve where biotite-muscovite granite forms. Local enrichments in Mn and B further crystallize garnet and tourmaline, respectively. The unique zonal pattern characterized by the occurrence of the evolved biotite-muscovite granite at the margin may be accounted for by the passive stoping during the emplacement of the Hongjesa granite. This emplacement may have occurred in continental collision environment, according to the tectonic discrimination diagram using major element chemistry.

Key Words : Hongjesa granite, biotite granite, biotite-muscovite granite, fractional crystallization, liquidus topology

INTRODUCTION

The Hongjesa granite is one of the well-known Precambrian granitoids in the Korean Peninsula, and occurs as batholith in the northeastern part of the Sobaeksan massif. The Hongjesa granite has received much attention because of its petrological characteristics such as the occurrence of bluish-grey K-feldspar, and its tectono-magmatic importance for unraveling the evolution of the Sobaeksan massif.

The Hongjesa granite covering the area of *ca.* 250-300 km^2 intrudes the Precambrian metasedimentary rocks, and is overlain by Cambro-Ordovician Chosun Supergroup (Fig. 1). The study area is located at Seokpo-ri, Bonghwa-kun in Kyeongsangbuk-do, Korea, enclosing western and central parts of the Hongjesa granite batholith. This area, in particular, has been the target for extensive geochemical and geochronological investigations (Na and Lee, 1978; Kim and Lee, 1983; Hong, 1985, 1992; Kim *et al.*, 1986; Chang *et al.*, 1988; Lee *et al.*, 1992; Park *et al.*, 1993).

Kim and Lee (1983) has divided the Hongjesa granite into four rock units. The study area belongs to the Precambrian Hongjesa granite gneiss according to their classification. Kim *et al.* (1986) have suggested that the Hongjesa granite is the S-type granite formed at compressional plate margin, and that the P-T conditions of the Hongjesa granite are 600-700℃ and 4-6 kbar, respectively. Chang *et al.* (1988) have suggested that the mineralogical and textural variations of the Hongjesa granite result from the different degree of partial melting. However, this hypothesis needs to be tested because their result is simply based on the small number of the analyzed samples. Hong (1985, 1992) has concluded that the

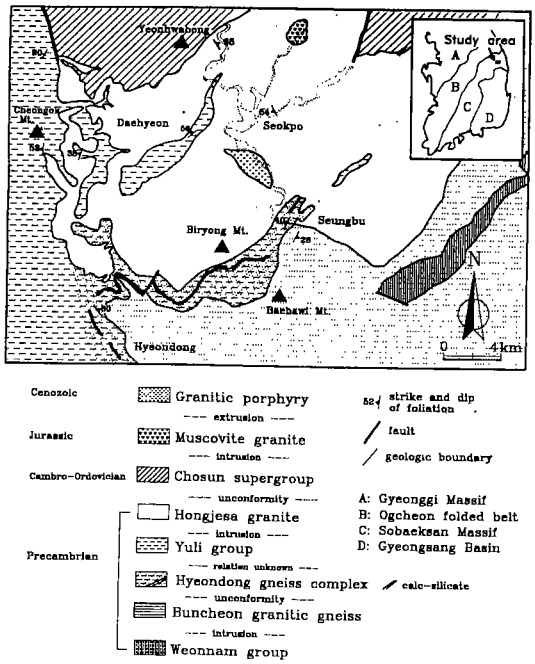

Fig. 1. Location and geologic map of the study area (modified after Kim and Lee, 1983).

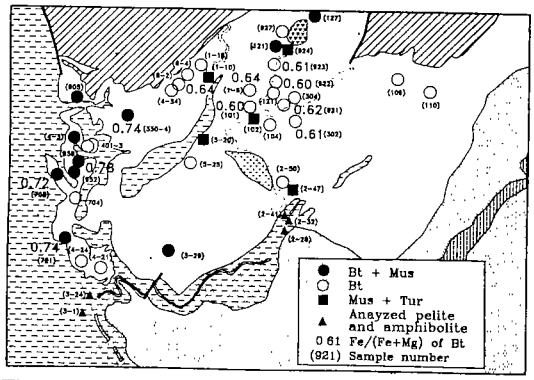

Fig. 2. Sample location map showing mineral assemblages of the Hongjesa granite and the X_{Fe} (=Fe/(Fe+Mg)) values of biotite in each sample.

Hongjesa granite is formed by partial melting of sedimentary source rocks, and the local chemical variation results from the variable degrees of fractional crystallization. In addition, he has reported that the Hongjesa granite has low magnetic susceptibility of the ilmenite series (Ishihara, 1977).

Whole rock Rb-Sr age of the Hongjesa granite is 1.71-1.83 Ga (Choo and Lee, 1980), whereas preliminary Pb-Pb age suggests 1.65 Ga (S.-T. Kwon, unpub. data). The Naedeogri and Nongkeori granites, petrographically similar to the Hongjesa granite, yield K-Ar muscovite ages of 1.64-1.79 and 1.59-1.80 Ga, respectively (Yun, 1983; Lee, 1988). The K-Ar biotite ages of the Hongjesa granite are divided into three age groups of 1.2-1.3, 0.6-0.7 and 0.3-0.4 Ga by Hong and Choi (1986). However, this grouping can be arbitrary because the isotopic effects of the surrounding Mesozoic granite are unknown.

Precambrian metasedimentary rocks in the study area have been referred to as the Yuli series (*e.g.*, Yun, 1967). Kim *et al.* (1986) divided the Yuli series into the Taekbaeksan schist complex and the Hyeondong schist complex on the basis of petrography and metamorphic grade. Kim (1991) further renamed the Hyeondong schist complex as the Hyeondong gneiss complex.

Most of previous studies of the Hongjesa granite have focused mainly on the geochemical aspects such as trace element, rare earth element (REE), and radiogenic isotope modelling without due attention to mineral assemblage and chemistry. The mineralogical aspect of the Hongjesa granite in the light of whole rock chemistry is the primary focus of our study. Thus we attempt (1) to determine both spatial distribution and compositional variation of primary rock-forming minerals; and (2) to delineate magmatic evolution on the basis of both mineral and whole rock chemistries of the Hongjesa granite. Subsolidus metamorphic relations of both the Hongjesa granite and the country rocks will be treated in the accompanying paper (Kim *et al.*, 1994).

GENERAL GEOLOGY

The Hongjesa granite intrudes the Precambrian metasedimentary rocks of the Hyeondong gneiss complex and the Yuli group rocks. Although grain size, color, and petrography of the granite are variable, biotite predominates as mafic phase in the central part, and both biotite and muscovite occur in the marginal part of the study area (Fig.

2). We designate these rock units as biotite granite and biotite-muscovite granite, respectively, although the boundary is not precisely determined yet. Muscovite-tourmaline granite sporadically occurs in the study area (Fig. 2). Jurassic muscovite granite defined by Kim and Lee (1983) occurs as a small stock in the northern area. This granite also contains minor tourmaline, but is finer-grained than muscovite-tourmaline granite. Pegmatites containing megacrysts of muscovite, tourmaline and grey K-feldspar commonly occur as veins and dykes near the boundary between the Hongjesa granite and the Yuli group. Towards the margin of the Hongjesa pluton occurs the migmatitic granite in which biotite-rich aggregates are aligned. Otherwise, migmatitic granite is similar in its appearance to other types of the Hongjesa granite.

Various rock types of the Yuli group and the Hyeondong gneiss complex occur as rounded xenoliths or roof-pendants at the marginal part of the Hongjesa granite. Thermal effect such as contact aureole or chilled margin is not distinct except for the partially-melted metasedimentary xenolith. Abundant xenoliths together with their sharp contact relationship indicate that the Hongjesa granite is a relatively shallow intrusion. Low-grade metamorphism of the Yuli group rocks and local development of migmatite corroborate the shallow depth origin. The absence of structural features compatible with metamorphic fabrics of country rocks suggests that the Hongjesa granite may be post-tectonic (Clarke, 1992).

The Buncheon granitic gneiss occurring in the southern part of the study area has no bluish-grey K-feldspar, and is well foliated in contrast to the Hongjesa granite. Thus, major deformation may have occurred prior to the intrusion of the Hongjesa granite. Because foliations commonly associated with the augen texture regionally develop (Kim *et al.*, 1991), deformational features of the Buncheon granitic gneiss cannot be attributed to the forceful injection of the Hongjesa granitic magma. The lack of regional deformational fabrics in the Hongjesa granite further suggests that high-temperature ductile deformation event was absent after the emplacement of the Hongjesa granite.

The Hyeondong gneiss complex located between the Hongjesa granite and the Buncheon granitic gneiss is composed of banded gneiss, migmatitic gneiss, quartzite and calc-silicate rock. The complex is characterized not only by the higher metamorphic grade than the Yuli group rocks but also by the occurrence of calc-silicate and amphibolitic rocks that are rare in the Yuli group. The Yuli group mainly consists of low-grade metasedimentary rocks containing chlorite porphyroblasts and mica pseudomorphs after andalusite and/or cordierite. The boundary between the Hyeondong gneiss complex and the Yuli group is not clearly defined yet. As a matter of fact, these two rock units can be identical in their lithology except for calc-silicate and amphibolite layers and differ only in their metamorphic grade.

Cambro-Ordovician Chosun Supergroup unconformably overlies the Hongjesa granite in the northern and central parts of the study area, and the Tertiary granitic porphyry intrudes the Hongjesa granite (Kim and Lee, 1983; Fig. 1).

PETROGRAPHY

The Hongjesa granitic batholith consists primarily of quartz, plagioclase, and K-feldspar together with minor biotite, muscovite, tourmaline, titanite, ilmenite, and pyrite. These minerals are euhedral to subhedral and mostly medium-grained. The most notable feature of the Hongjesa granite is the occurrence of bluish-grey K-feldspar megacryst. Trace amounts of garnet and sillimanite rarely occur in biotite-muscovite granites. The modal percentage of biotite ranges from 2% to 18%, while that of muscovite ranges from 1% to 5% in biotite-muscovite granite. Muscovite occurs as both coarse platy crystals and as aggregates of fine ragged crystals. The phenocrysts of garnet rarely occur in one biotite-muscovite granite in contact with the Yuli group. Apatite and zircon are commonly observed as minor phase.

The linear arrangement of biotite is uncom-

monly observed in the Hongjesa granitic body. This fabric is not magmatic, because other primary minerals such as K-feldspar and plagioclase are randomly oriented and ductile deformations such as inter- or intra-crystalline fractures of plagioclase are absent (Paterson *et al.*, 1989; John and Blundy, 1993). Thus, the linear fabric of biotite may result from the subsolidus deformation.

Many xenoliths of pelitic, psammitic and basaltic compositions occur along the margin of the pluton, while they are absent inward. These xenoliths are derived from both the Yuli group and the Hyeondong gneiss complex. Most xenoliths are rounded or ellipsoidal in shape, and range from a few cm to 3-4 m in the maximum dimension. Two representative types of metasedimentary xenoliths are: (1) meta-sandstone and -siltstone consisting primarily of equigranular aggregates of quartz and sericitized plagioclase with minor biotite; and (2) surmicaceous enclaves (Montel *et al.*, 1991) consisting of biotite, muscovite, K-feldspar, quartz and opaque minerals. Sillimanite is often present as prismatic crystal and fibrous mat in the surmicaceous enclave. Because amphibolite occurs in the Hyeondong gneiss complex, the occurrence of amphibolitic xenoliths corroborates the field evidence that the Hongjesa granite intrudes the Hyeondong gneiss complex. Mineral assemblages of the amphibolitic xenoliths are different from those of the Hyeondong gneiss complex because of the intensive retrogression. The major constituent minerals are garnet, hornblende, quartz, epidote and biotite. Neither dark mafic microgranular enclaves representing the interaction between mafic and felsic magmas (Holden *et al.*, 1987), nor restitic xenoliths containing high-grade assemblages and textures such as granoblastic texture, foliated fabric and zoned plagioclase (Wall *et al.*, 1987) are found.

ANALYTICAL METHODS

About three hundred samples of granite and metasedimentary rocks were collected and petrographically examined. Major elements of fifteen granites together with five metasedimentary and amphibolitic rocks were analyzed on glass plates of fused rock samples by X-ray fluorescent spectrometer (Phillips PW1480) at the Korean Basic Science Center. Representative whole rock compositions and the CIPW norms are given in Table 1.

The chemistries of rock-forming minerals in twenty-four samples were determined using the JEOL 733A electron microprobe at Seoul National University. The whole set of analytical data is available in Kim (1994). For further analytical conditions, refer to Lee and Cho (1992).

BULK ROCK CHEMISTRY

The SiO_2 content of the Hongjesa granite considerably varies from 61.6 to 75.9 wt%, but mostly ranges from 70.6 to 75.9 wt% except for two samples 921 and 923 (Table 1). As apparent from the occurrence of muscovite, garnet and tourmaline, the Hongjesa granite is moderately to strongly peraluminous and its normative corundum ranges from 1.43 to 4.60 wt%. The contents of SiO_2 and normative corundum do not systematically vary with sample locations in the study area.

The peraluminous chemistry of the Hongjesa granite may result from: (a) partial melting of peraluminous sedimentary rocks; (b) differentiation of metaluminous magma; and (c) late-stage but super-solidus metasomatic loss of alkalis via vapor phase (Zen, 1986, 1988; Clarke, 1992). The fractionation of metaluminous parent magma is generally insufficient to produce a large mass of peraluminous melt (Speer, 1987; Zen, 1988). If alkalis were transported by vapor phase, relict metaluminous minerals should occur with the alkali and volatile-rich phases. However, such evidences are not found in the Hongjesa granite. The Hongjesa granite is likely to be the product of partial melting of meta-sedimentary rocks, primarily because of high Al content of biotite and high initial $^{87}Sr/^{86}Sr$ ratio of 0.717-0.723 (Choo and Lee, 1980).

The variations of major elements of this study and Lee *et al.* (1992) are shown in the Harker diagram (Fig. 3). Compositional trends of each

Table 1. Major element oxides (wt%) and CIPW normative minerals of the Hongjesa granite and the country rocks

	Biotite granite					Biotite-muscovite granite				A	Muscovite-tourmaline granite				B	Country rocks				
	1-6	227	921	922	923	708	709	721	905	958	1-10	5-20	102	924	4-1	2-41	3-1	2-26	2-32	3-24
SiO_2	70.59	72.55	64.30	72.28	61.56	72.34	75.89	72.98	74.40	74.66	75.33	74.22	74.50	72.54	74.28	54.27	62.37	51.33	52.91	56.86
TiO_2	0.48	0.17	0.49	0.21	0.72	0.16	0.03	0.15	0.12	0.06	0.07	0.02	0.07	0.06	0.30	0.85	0.60	0.77	1.73	0.63
Al_2O_3	13.61	14.08	16.81	13.74	17.57	14.44	13.76	14.59	14.41	13.72	14.57	14.97	14.31	15.11	13.38	20.06	18.10	13.42	12.59	11.75
Fe_2O_3	4.52	2.42	4.53	2.49	6.17	3.01	0.90	2.23	1.82	2.03	1.10	1.62	1.52	2.17	3.89	9.41	7.53	13.13	16.97	20.61
MnO	0.05	0.02	0.04	0.02	0.05	0.03	0.01	0.02	0.02	0.07	0.01	0.01	0.02	0.03	0.04	0.10	0.06	0.18	0.27	0.09
MgO	1.19	0.45	1.29	0.60	1.89	0.33	0.07	0.37	0.26	0.17	0.24	0.11	0.20	0.33	1.05	3.90	2.49	7.26	5.14	5.59
CaO	2.21	1.45	2.38	0.72	2.80	0.85	1.09	0.89	0.66	0.79	0.36	0.58	0.45	0.60	0.93	1.37	0.14	9.69	3.50	2.69
Na_2O	3.71	3.44	3.07	1.96	3.63	2.19	4.02	2.99	2.11	2.37	3.40	6.16	2.95	3.98	2.91	2.25	0.31	2.60	0.76	0.55
K_2O	1.96	4.16	4.57	6.88	3.34	5.61	3.78	4.75	5.14	5.33	3.79	1.09	5.11	3.94	2.29	4.27	5.58	0.40	3.63	0.48
P_2O_5	0.03	0.08	0.26	0.09	0.30	0.20	0.09	0.10	0.16	0.07	0.16	0.25	0.22	0.29	0.09	0.10	0.08	0.07	0.17	0.07
L.O.I	1.23	0.98	1.77	0.87	1.77	0.65	0.22	0.85	0.72	0.52	0.78	0.50	0.51	0.68	0.52	2.88	2.48	0.75	1.57	0.28
Total	99.58	99.80	99.51	99.86	99.80	99.81	99.86	99.92	99.82	99.79	99.81	99.53	99.86	99.73	99.98	99.46	99.74	99.60	99.24	99.60
Qtz	35.07	33.04	22.59	32.34	19.60	36.32	35.83	35.20	41.06	38.71	40.32	33.44	37.08	33.27	45.26					
C	1.43	1.45	3.05	1.95	3.54	3.65	1.27	3.13	4.52	2.77	4.57	3.14	3.58	3.83	4.60					
Or	11.58	24.59	27.01	40.66	19.74	33.15	22.34	28.07	30.38	31.50	22.40	6.44	30.20	23.28	13.53					
Ab	31.39	29.11	25.98	16.59	30.72	18.53	34.02	25.30	17.86	20.06	28.77	52.13	24.96	33.68	24.63					
An	10.79	6.72	10.28	3.04	12.13	3.04	4.88	3.83	2.33	3.51	0.85	1.41	0.94	1.27	4.09					
En	2.96	1.12	3.21	1.50	4.71	0.82	0.17	0.92	0.65	0.42	0.60	0.27	0.50	0.82	2.62					
Il	0.11	0.04	0.09	0.04	0.11	0.06	0.02	0.04	0.04	0.06	0.02	0.02	0.04	0.06	0.09					
Ap	0.07	0.19	0.62	0.21	0.71	0.47	0.21	0.24	0.38	0.17	0.38	0.59	0.52	0.69	0.21					
Hem	4.52	2.42	4.53	2.49	6.17	3.01	0.90	2.23	1.82	0.11	1.10	1.62	1.52	2.17	3.89					
Rut	0.42	0.15	0.45	0.19	0.66	0.13	0.02	0.13	0.10	1.99	0.06	0.01	0.05	0.03	0.26					
D.I.	78.05	86.74	75.57	89.58	70.06	88.01	92.18	88.58	89.29	90.26	91.49	92.01	92.24	90.23	83.42					

A=Garnet-bearing biotite-muscovite granite; B=Migmatitic granite; D.I. represents the sum of normative Qtz+Ab+Or.

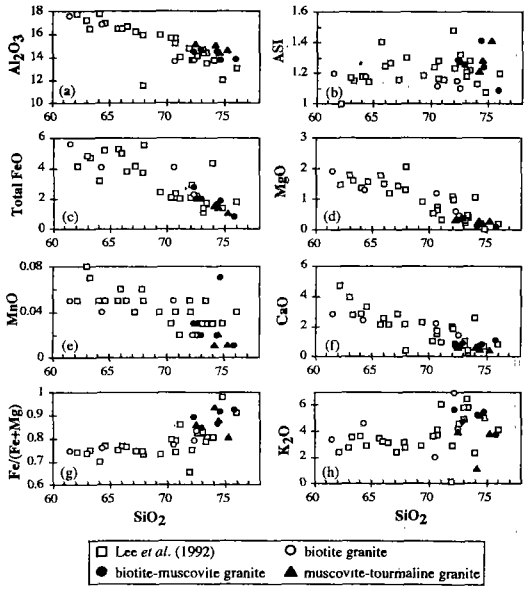

Fig. 3. The Harker diagrams showing the variation in major oxides, ASI values and Fe/(Fe+Mg) ratios of the Hongjesa granite. Symbols: open circle, biotite granite in the Seokpo area; closed circle, biotite-muscovite granite in the Daehyeon area; filled triangle, muscovite-tourmaline granite; and open square, granites analyzed by Lee *et al.* (1992).

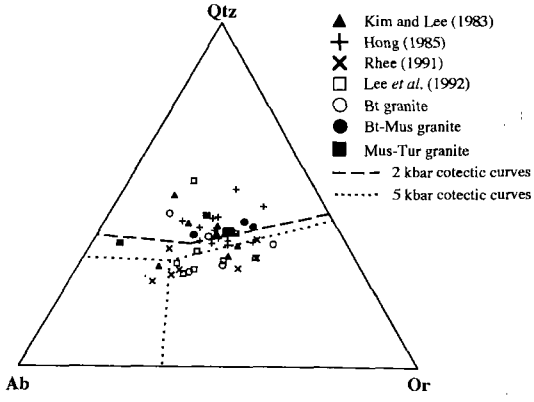

Fig. 4. Ternary diagram of quartz (Qtz)-orthoclase (Or)-albite (Ab), showing the normative mineralogy of the Hongjesa granite. Dashed and dotted lines respectively represent the 2 kbar and 5 kbar cotectic curves in the haplogranitic system (Holtz *et al.*, 1992).

oxide except K_2O are generally continuous. It is thus apparent that the fractional crystallization has governed the formation of each granite type in the Hongjesa pluton. The Al_2O_3 content decreases with increasing SiO_2 (Fig. 3a), implying the continuous crystallization of feldspar. The aluminum saturation index (ASI) defined by molar $Al_2O_3/(CaO+Na_2O+K_2O)$ (Shand, 1951; Zen, 1986) does not systematically vary with SiO_2 (Fig. 3b). However, the ASI values of biotite-muscovite and muscovite-tourmaline granites are greater than those of biotite granite.

The total FeO, MgO and MnO contents decrease with increasing SiO_2 content (Fig. 3c, d and e). This trend is attributed to the continuous crystallization of biotite. On the other hand, the decrease of Ca content with increasing SiO_2 (Fig. 3f) is accounted for by the fractionation of plagioclase. The X_{Fe} (= Fe/(Fe+Mg)) value is fairly constant below 70 wt% SiO_2, but steadily increases above 70 wt% SiO_2 (Fig. 3g). The K_2O content is nearly constant below 70 wt% SiO_2, but tends to be enriched at higher SiO_2 values. The alkali enrichment by the K-metasomatism is not likely, as discussed in a later section. In total alkalis-FeO-MgO diagram (Kim, 1994), the analyzed bulk compositions of the Hongjesa granite belong to the calc-alkaline fractionation trend. In summary, all of the results in Fig. 3 suggest that the fractional crystallization is important for chemical variation of the Hongjesa granite, and that biotite-muscovite and muscovite-tourmaline granites are more evolved than biotite granite.

The bulk rock chemistry of the Hongjesa granite can be approximated by the quartz-albite-orthoclase-H_2O system, because the sum of normative feldspars and quartz is greater than 85% (Table 1). Fig. 4 is a ternary plot of normative quartz, albite and orthoclase, compiled from the analytical data available for the Hongjesa granite (Kim and Lee, 1983; Hong, 1985; Rhee, 1991; Lee *et al.*, 1992). Ternary minima and cotectic curves of the haplogranite system at 2 and 5 kbar (Holtz *et al.*, 1992) are also shown. When all the available data are taken into account, the normative composition of the Hongjesa granite is highly variable (Fig. 4). However, biotite-muscovite granite appears to contain more normative quartz than biotite granite. Thus the former may have been emplaced at lower pressure than the latter. However, the estimation of pressure based on Fig.

4 is not warranted in the absence of the quantitative data on B and F contents, CO_2 fugacity of fluid, and the An content of plagioclase (Winkler, 1979; Manning and Pichavant, 1988).

MINERALOGY AND MINERAL CHEMISTRY

Quartz

Quartz in the Hongjesa granite is anhedral and shows undulatory extinction. The longest dimensions of quartz are mostly less than 2-3 mm. The grain boundary between quartz and other minerals is embayed or straight, whereas that between quartz crystals is lobate or sutured. The latter may result from weak post-crystalline deformation (Spry, 1969). Rounded or euhedral quartz grains occur as inclusions in plagioclase and K-feldspar.

Plagioclase

Plagioclase grains are commonly euhedral and partly altered. Alteration is most prominent at the An-rich core or along the cleavage plane of plagioclase. Sericitization and saussuritization are ubiquitous, and produce albitic plagioclase (An_{1-5}) commonly as overgrowth on primary oligoclase, together with muscovite, epidote, carbonate and opaque minerals (Fig. 5a). The albitic rim is prominent in plagioclase grains neighboring K-feldspar.

The compositions of plagioclase grains in biotite granite range from An_{17} to An_{28} (Table 2), and most of these grains show little or weak zoning with Na-rich rim. The normal zoning in one plagioclase grain is represented by continuous compositional change, ranging from An_{28} at the core to An_{17} at the rim. The zoning pattern of plagioclase is often visible optically by variable degree of alteration. The composition of plagioclase in biotite-muscovite granite is An_{11-18} (Table 2). The patterns of zoning and alteration are similar to those of biotite granite. Plagioclase grains in both muscovite-tourmaline granite and Jurassic muscovite granite are albitic (An_{2-5}) and show no compositional zoning.

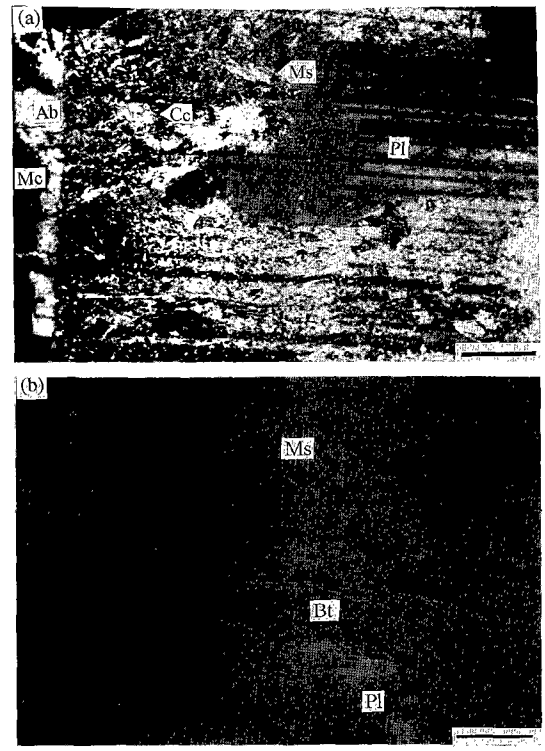

Fig. 5. Photomicrographs of the Hongjesa granite: (a) partially saussuritized plagioclase showing the albitic rim towards microcline (sp. 922); (b) coexisting biotite and muscovite in biotite-muscovite granite in sp. 4-3. The scale bars represent 0.5 mm. Abbreviations: Ab, albite; Bt, biotite; Cc, carbonate; Mc, microcline; Ms, muscovite; and Pl, plagioclase.

The higher An content of biotite granite than that of biotite-muscovite granite is consistent with the variation in the CaO content of whole rock (Fig. 3f). The An content of plagioclase, however, does not systematically vary among each granite types. This phenomenon is partly attributed to the subsolidus recrystallization of plagioclase.

K-feldspar

K-feldspar occurs not only as euhedral to subhedral megacryst of perthite and microcline but also as interstitial groundmass phase. In some pegmatites, the maximum dimension of bluish-grey K-feldspar reaches 20 cm. Most K-feldspar grains are exsolved into nearly pure K-feldspar

Table 2. Representative analyses of plagioclase

	Biotite granite					Biotite-muscovite granite				A	B	C	
	213-31	227-9	921-25	922-16	923-13	708-13	709-10	721-11	905-14	958-A	4-1-31	102-9	924-20
SiO_2	60.24	62.10	59.29	63.92	61.93	62.84	65.82	63.79	62.85	63.95	62.45	67.03	67.61
Al_2O_3	25.17	24.27	25.83	22.39	24.58	23.11	21.19	23.20	22.02	22.85	23.76	20.74	20.03
TiO_2	0.00	0.00	0.00	0.02	0.02	0.00	0.04	0.00	0.00	0.01	0.03	0.01	0.01
FeO	0.00	0.03	0.00	0.04	0.00	0.05	0.07	0.02	0.00	0.04	0.00	0.05	0.00
MgO	0.00	0.01	0.00	0.01	0.00	0.00	0.00	0.01	0.00	0.01	0.00	0.00	0.00
MnO	0.00	0.05	0.02	0.00	0.00	0.00	0.00	0.00	0.02	0.00	0.02	0.00	0.00
CaO	6.04	4.96	7.22	3.84	5.50	3.66	2.50	4.03	3.22	3.27	4.60	1.09	0.40
Na_2O	8.45	8.85	7.55	9.72	8.55	9.99	10.90	9.91	9.93	10.51	8.86	11.42	11.86
K_2O	0.20	0.32	0.17	0.18	0.22	0.20	0.06	0.14	0.19	0.00	0.26	0.15	0.10
Total	100.10	100.59	100.08	100.12	100.80	99.85	100.58	101.10	98.23	100.64	99.98	100.49	100.01
Number of cations on the basis of 8 oxygens													
Si	2.680	2.740	2.642	2.822	2.726	2.788	2.885	2.793	2.826	2.810	2.765	2.927	2.961
Al	1.321	1.263	1.358	1.166	1.277	1.209	1.096	1.199	1.169	1.184	1.241	1.069	1.035
Subtotal	4.001	4.003	4.000	3.988	4.003	3.997	3.991	3.992	3.995	3.994	4.006	3.996	3.996
Ti	0.000	0.000	0.000	0.001	0.001	0.000	0.001	0.000	0.000	0.000	0.001	0.000	0.000
Fe	0.000	0.001	0.000	0.001	0.000	0.002	0.003	0.001	0.000	0.001	0.000	0.002	0.000
Mg	0.000	0.001	0.000	0.001	0.000	0.000	0.000	0.001	0.000	0.001	0.000	0.000	0.000
Mn	0.000	0.002	0.001	0.000	0.000	0.000	0.000	0.000	0.001	0.000	0.001	0.000	0.000
Ca	0.288	0.234	0.345	0.182	0.259	0.174	0.117	0.189	0.155	0.154	0.218	0.051	0.019
Na	0.729	0.757	0.652	0.832	0.730	0.859	0.926	0.841	0.866	0.895	0.761	0.967	1.007
K	0.011	0.018	0.010	0.010	0.012	0.011	0.003	0.008	0.011	0.000	0.015	0.008	0.006
Subtotal	1.028	1.013	1.008	1.027	1.002	1.046	1.050	1.040	1.033	1.051	0.996	1.028	1.032
An	28.0	23.2	34.3	17.4	25.9	16.7	11.2	18.2	15.1	14.7	22.0	5.0	1.8
Ab	70.9	75.0	64.8	81.3	72.9	82.3	88.5	81.1	83.9	85.3	76.5	94.2	97.6
Or	1.1	1.8	1.0	1.0	1.2	1.1	0.3	0.7	1.0	0.0	1.5	0.8	0.5

A=Garnet-bearing biotite-muscovite granite; B=Migmatitic granite; C=Muscovite-tourmaline granite; An=100×Ca/(Ca+Na+K); Ab=100×Na/(Ca+Na+K); Or=100×K/(Ca+Na+K).

(Or_{96-99}) and albite (An_{1-2}). Secondary rod-like K-feldspar (Or_{99}) also occurs along the cleavage plane of biotite in association with chlorite.

The K-feldspar megacrysts contain abundant inclusions, primarily consisting of plagioclase, quartz and muscovite, and rarely of biotite. This textural relationship indicates that K-feldspar crystallized at the late magmatic stage. Fine-grained inclusions of plagioclase in K-feldspar are commonly rimmed by albite accompanying the sericitization. The texture is previously referred to as "island and sea" texture produced by K-metasomatism (Kim and Lee, 1983; Kim *et al.*, 19 86). It should be noted, however, that the evidence for K-metasomatism is superficial (see below for further discussion).

Biotite

Biotite occurs as reddish to reddish brown, euhedral to anhedral crystal, and defines the local foliation in the Hongjesa granite. Its long dimension varies from 0.1 mm to 3 mm. Biotite is commonly replaced by chlorite and muscovite in association with minute grains of K-feldspar.

The X_{Fe} values of biotite range from 0.58 to 0.78, and systematically vary with the type of granite (Fig. 6a; Table 3). Most of the X_{Fe} values of biotite granite are significantly smaller than those of biotite-muscovite granite. The average X_{Fe} value of biotite granite is 0.62, but that of biotite-muscovite granite is 0.74. Biotite of garnet-bearing biotite-muscovite granite has the highest X_{Fe} value of 0.78.

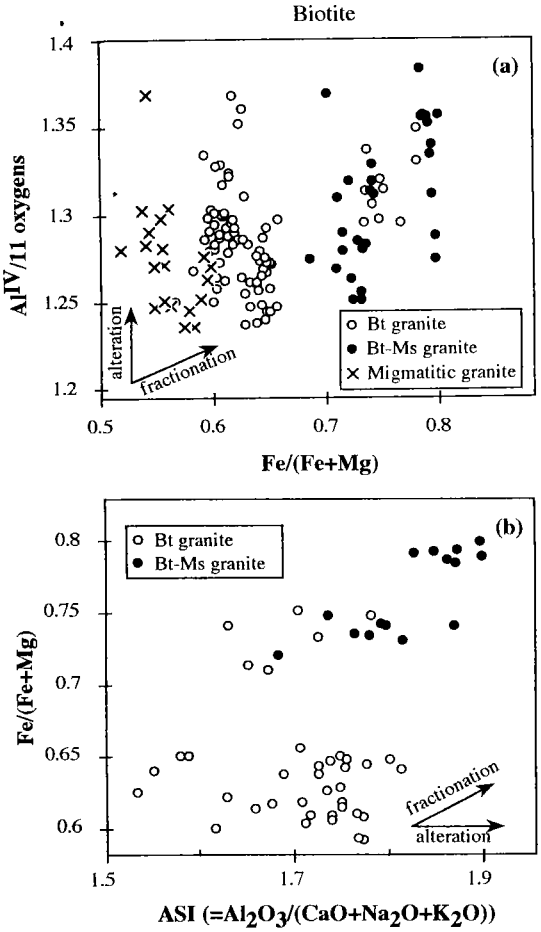

Fig. 6. Composition of biotite plotted in terms of: (a) Al^{IV} and Fe/(Fe+Mg); and (b) Fe/(Fe+Mg) and the ASI value based on 11 anhydrous oxygens. Two vectors represent the compositional changes of biotite predicted for fractional crystallization and subsolidus alteration, respectively.

The Al^{IV} content of biotite is variable even in one single sample, although the X_{Fe} value is fairly constant. This variation is attributed to the subsolidus alteration of biotite. The constant X_{Fe} value of biotite within a sample indicates that the X_{Fe} value does not significantly change during the alteration of biotite (Fig. 6). Biotite of migmatitic granite has distinctly lower X_{Fe} values (0.51-0.65) than those of other biotite granites. Hence, its origin may be different from that of biotite and biotite-muscovite granites.

The X_{Fe} and ASI values (Table 3) of biotite are plotted in Fig. 6b. To minimize the effect of alteration, biotites with the K content greater than 0.9 cations per formula unit (p.f.u.) on 11 anhydrous oxygen basis are only considered. The X_{Fe} and ASI values of biotite concomitantly increase from biotite granite to biotite-muscovite granite. The ASI value of biotite from biotite-muscovite granite is greater than that from biotite granite, as found in the whole rock analysis (Fig. 3b). As the ASI value of biotite reflects the alumina activity in magma (Zen, 1988), the Al enrichment in biotite is attributed to the fractionation of magma. Guidotti (1984) has suggested that the composition of biotite may not change at the metamorphic grade lower than the amphibolite facies. Because high grade metamorphism above the amphibolite facies is not observed after the emplacement of the Hongjesa granite, the compositional change of biotite is not likely to result from metamorphic reactions. Hence, the increases in X_{Fe} values and Al contents of biotite (Fig. 6) are attributed to the different degree of fractional crystallization in the Hongjesa granitic magma.

Muscovite

Muscovite of the Hongjesa granite is either primary or secondary. Primary muscovite occurs as coarse-grained euhedral phenocryst or as embayed crystal intergrown with biotite (Fig. 5b) in biotite-muscovite and muscovite-tourmaline granites. Most primary muscovites satisfy the compositional and textural criteria suggested by Miller *et al.* (1981). Secondary muscovite occurs along the rim or cleavage plane of biotite and as the product of sericitization or saussuritization of plagioclase in biotite and biotite-muscovite granite. Further compositional details of muscovite are discussed in the accompanying paper (Kim *et al.*, 1994).

Tourmaline

Tourmaline coexists with muscovite in five samples of muscovite-tourmaline granite as well as Jurassic muscovite granite (Fig. 2). The X_{Fe} value of

Table 3. Representative analyses of biotite

	Biotite granite						Biotite-muscovite granite				A	B	
	6-2-97	213-32	227-47	921-18	922-12	923	708-2	709-17	721-15	905-7	958-40	4-1-1	808-26
SiO_2	34.27	34.33	34.76	34.91	35.35	35.16	32.93	34.35	34.02	33.96	32.86	34.96	35.11
Al_2O_3	18.34	19.58	18.35	18.76	17.80	17.57	19.68	18.50	18.74	18.04	19.16	18.15	19.15
TiO_2	1.08	2.80	1.69	2.78	1.73	2.55	1.23	1.67	2.02	1.72	1.93	1.80	2.21
FeO(T)	22.75	19.83	24.31	20.59	20.73	21.83	26.16	25.18	25.51	24.79	26.27	19.86	18.86
MgO	6.99	7.19	6.28	7.44	7.66	7.37	4.03	5.17	4.97	4.80	4.14	8.99	9.15
MnO	0.22	0.16	0.10	0.23	0.09	0.11	0.26	0.26	0.06	0.30	0.25	0.50	0.15
CaO	0.01	0.02	0.11	0.02	0.00	0.37	0.02	0.00	0.03	0.05	0.02	0.01	0.08
Na_2O	0.05	0.11	0.02	0.15	0.08	0.07	0.04	0.11	0.05	0.04	0.03	0.05	0.00
K_2O	9.33	8.74	9.23	9.83	9.49	9.85	9.62	9.23	9.53	8.01	8.46	9.79	9.62
Total	93.04	92.76	94.85	94.71	92.93	94.88	93.97	94.47	94.93	91.71	93.12	94.11	94.33
Number of cations on the basis of 11 anhydrous oxygens													
Si	2.726	2.672	2.725	2.701	2.781	2.736	2.644	2.720	2.688	2.744	2.651	2.718	2.697
Al^{IV}	1.274	1.328	1.275	1.299	1.219	1.264	1.356	1.280	1.312	1.256	1.349	1.282	1.303
Subtotal	4.000	4.000	4.000	4.000	4.000	4.000	4.000	4.000	4.000	4.000	4.000	4.000	4.000
Al^{VI}	0.448	0.469	0.421	0.413	0.434	0.348	0.508	0.448	0.435	0.463	0.475	0.384	0.432
Ti	0.065	0.164	0.099	0.162	0.102	0.149	0.074	0.099	0.120	0.104	0.117	0.105	0.128
Fe	1.513	1.291	1.593	1.332	1.364	1.420	1.756	1.667	1.686	1.674	1.772	1.291	1.211
Mg	0.829	0.834	0.734	0.858	0.898	0.854	0.482	0.610	0.585	0.578	0.498	1.041	1.047
Mn	0.015	0.011	0.006	0.015	0.006	0.007	0.017	0.018	0.004	0.020	0.017	0.033	0.010
Subtotal	2.870	2.769	2.853	2.780	2.804	2.778	2.837	2.842	2.830	2.839	2.879	2.854	2.828
Ca	0.001	0.002	0.009	0.002	0.000	0.031	0.001	0.000	0.002	0.004	0.002	0.001	0.007
Na	0.008	0.017	0.004	0.023	0.011	0.011	0.007	0.017	0.008	0.007	0.006	0.008	0.000
K	0.946	0.867	0.922	0.970	0.952	0.978	0.985	0.933	0.961	0.825	0.870	0.971	0.942
Subtotal	0.955	0.886	0.935	0.995	0.964	1.019	0.993	0.949	0.971	0.836	0.878	0.980	0.949
ASI	1.799	2.023	1.793	1.717	1.713	1.533	1.872	1.819	1.792	2.043	2.068	1.696	1.814
Fe/(Fe+Mg)	0.646	0.607	0.685	0.608	0.603	0.624	0.785	0.732	0.742	0.743	0.781	0.554	0.536

A=Garnet-bearing biotite-muscovite granite; B=Migmatitic granite; ASI=molar $Al_2O_3/(CaO+Na_2O+K_2O)$.

schorlitic tourmaline ranges from 0.56 to 0.78. The coexistence of tourmaline with muscovite characterizes the peraluminous nature of granite. Tourmaline never coexists with biotite in the Hongjesa granite. These observations are consistent with the suggestion of Benard *et al.* (1984) that tourmaline is favored in strongly peraluminous magma.

In migmatitic granite, tourmaline rarely coexists with biotite and has the X_{Fe} value of 0.35-0.37. The low X_{Fe} value is in contrast with that of muscovite-tourmaline granite, but consistent with that of the Yuli group. Thus, tourmaline in migmatitic granite may be inherited from metasedimentary country rock

Garnet

Garnet occurs as minute grains in two samples of biotite granite and as phenocrysts in one garnet-bearing biotite-muscovite granite (sp. 958) ranging up to 1 cm in the maximum dimension. Both types of garnet have nearly identical composition of $\sim Alm_{80}Sps_{13}Pyp_4Grs_3$, and are commonly replaced by chlorite along the fracture. The garnet is not likely to be metamorphic, because garnet is absent in the Yuli group and its composition is different from that of the Hyeondong gneiss complex ($Alm_{65}Sps_{11}Pyp_8Grs_{16}$). The composition of garnet in the Hongjesa granite is different from that of typical magmatic Mn-rich

garnet (Allan and Clarke, 1981; Miller and Stoddard, 1981; Kontak and Corey, 1988). However, not only the systematic variation in the X_{Fe} value of Fe-rich biotite coexisting with garnet, but also the highly evolved characteristics of bulk rock composition of garnet-bearing biotite-muscovite granite suggest that the origin of garnet is magmatic.

DISCUSSION

Fractional crystallization of the Hongjesa granite

Variation in the mineral assemblage of granite can be accounted for by several geological processes such as fractional crystallization, partial melting, assimilation, magma mixing, or subsolidus alteration. In particular, fractional crystallization may produce the systematic change in ferromagnesian minerals of granite: *e.g.*, biotite → biotite + muscovite → biotite + muscovite + garnet → tourmaline + muscovite (Abbott, 1985; Shearer *et al.*, 1987). In addition, the compositions of both principal and accessory phases such as the An content of plagioclase and the X_{Fe} values of mafic minerals systematically vary with fractionation (Tindle and Pearce, 1983; Shearer *et al.*, 1987; Speer and Becker, 1992). Such variations are observed in the Hongjesa granite: biotite granite primarily occurs in central part of the pluton, and biotite-muscovite granite in marginal part. Garnet-bearing biotite-muscovite granite occurs in one locality at the margin of the pluton, and muscovite-tourmaline granite sporadically occurs in the study area.

The systematic variations in mineral chemistry and assemblage of the Hongjesa granite may be rationalized using the AFM diagram of Fig. 7, where $A=Al_2O_3-CaO-Na_2O-K_2O$; $F=FeO+MnO$; and $M=MgO$ (Abbott and Clarke, 1979; Abbott, 1981). The tie-lines between biotite and muscovite shift towards the A-F side as mineral assemblages (+quartz, K-feldspar, and plagioclase) change from biotite through biotite + muscovite to biotite + muscovite + garnet. In addition, the X_{Fe} value of biotite increases from biotite granite through

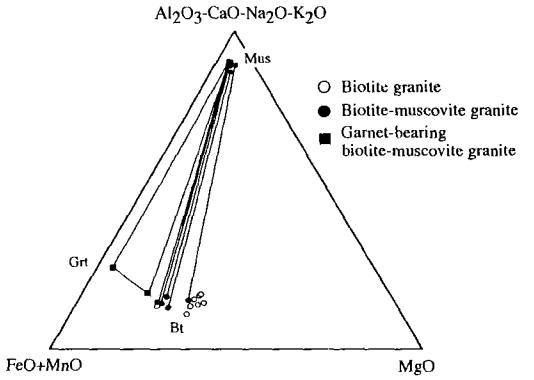

Fig. 7. An AFM diagram showing the analyzed compositions of biotite, muscovite, and garnet. Tie lines connect the compositions of the coexisting phases.

biotite-muscovite granite to garnet-bearing biotite-muscovite granite. This systematic change in the X_{Fe} value suggests that both biotite and muscovite are primary. Furthermore, in spite of the subsolidus equilibration, the An content of plagioclase in biotite-muscovite granite is smaller than that in biotite granite. These relationships are consistent with the fractional crystallization of the Hongjesa granitic magma, and corroborate the fact that the X_{Fe} value of biotite increases with fractionation in the granitic pluton (Leake, 1974; Mahmood, 1983; Speer, 1984).

The assimilation of granite with country rock may account for the compositional variation in ferromagnesian minerals of the Hongjesa pluton. However, the change in mineral assemblages at the marginal part of the pluton may not wholly result from the assimilation, because the addition of crustal materials into granitic magma will not drastically change the composition of a fractionating system (McBirney, 1979; Pitcher, 1993). In addition, the emplacement pressure of the Hongjesa granite is 3 ± 1 kbar corresponding to the depth of ~10 km (Kim *et al.*, 1994). The extensive assimilation is unlikely to occur because of the insufficient heat carried by a shallow-depth granitic intrusive (Ayuso and Arth, 1992). Field evidences such as the partial melting in xenoliths and the occurrence of migmatitic granite suggest that local assimilation has occurred. However, the

regional variations in mineral assemblage and chemistry as well as bulk rock composition are well accounted for by fractionation or probably assimilation-fractional-crystallization process. The trace element modelling of the Hongjesa granite (see below) corroborates the fractionation model. Further geochemical studies using trace or isotope elements are needed to evaluate the importance of possible assimilation for the evolution of the Hongjesa granite.

Kim and Lee (1983) and Lee *et al.* (1992) have suggested that K-metasomatism accompanying granitization is important for the petrogenesis of the Hongjesa granite. However, the granitization in a strict sense has not occurred in the Hongjesa granite. In case of granitization, Na, Al and Si should be introduced into granite, while Fe, Mg and Ca migrate away to the country rock (Kresten, 1988). As a result, the boundary between granite and the surrounding rock may be diffuse, and basic front concentrated with the mafic component should exist. In addition, the granitization may not produce any magmatic texture. However, in the Hongjesa granite, such a basic front is absent and the igneous textures are ubiquitous.

Trace element modelling of fractionation

As a first step for deciphering the evolutionary process of the Hongjesa granite, the variation diagrams of trace elements are useful to assess the relative importance of fractional crystallization *vs.* partial melting (*e.g.*, McCarthy and Hasty, 1976; Hanson, 1978; Brown *et al.*, 1981; Tindle and Pearce, 1981; Ayuso and Arth, 1992). We use the analytical data of Rb, Sr and Ba (Kim *et al.*, 1989) in order to model the petrogenesis of the Hongjesa granite. These elements are particularly useful because they are primarily concentrated in major silicate minerals of granite.

The trace element data of the Seokpo and Daehyeon areas are presented in Sr-Rb and Ba-Rb logarithmic plots of Fig. 8. The Seokpo area mainly consists of biotite granite, whereas biotite-muscovite granite occurs in the Daehyeon area. We have used a biotite granite sample with the highest Sr and Ba concentrations as the reference point representing the initial magma composition for fractional crystallization. For partial melting, however, the vectors are only schematic, because the reference point for the source rock composition is not available. The concentrations of each element are calculated at each step using Rayleigh fractionation and batch melting models defined as $C^L/C^O=F^{D-1}$ and $C^L/C^O=1/(F+D-F\cdot D)$, respectively, where C^L=concentration of a given element in the residual melt, C^O=concentration of the element in the original melt, F=fraction of melt formed by melting or melt remaining during fractionation, and D=bulk distribution coefficient (Hanson, 1978). Bulk dis-

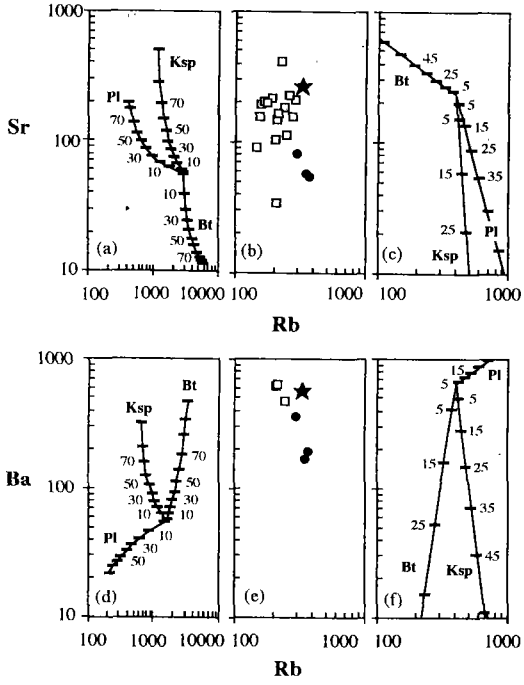

Fig. 8. The Sr-Rb and Ba-Rb relationships of the Hongjesa granite (data from Kim *et al.*, 1989). Theoretical vectors are calculated for partial melting (a and d), and fractionation (c and f) of biotite, plagioclase, and K-feldspar, respectively. The numbers on the vectors refer to the percentages of fractionation or partial melting. Note the different scale for the Rb concentration in case of partial melting. Star represents the reference point used for calculating the vectors in fractional crystallization. Symbols: open square, the Seokpo area; filled circle, the Daehyeon area.

tribution coefficients are from the compilation of the NEWPET computer program (Clarke, 1992). The result is shown in Fig. 8, where the melt compositions continuously change with Rayleigh fractionations or simple batch meltings of biotite, K-feldspar and plagioclase, respectively.

If fractional crystallization is responsible for the geochemical evolution of the Hongjesa granite, biotite together with plagioclase or K-feldspar are major fractionating phases in order to produce the observed trends in the Sr-Rb and Ba-Rb diagrams. In this case, biotite-muscovite granite in the Daehyeon area is more evolved than biotite granite in the Seokpo area.

Alternatively, if partial melting predominates, either K-feldspar and plagioclase or K-feldspar and biotite are the melting phases necessary for the Sr-Rb or Ba-Rb variation, respectively. Such a discrepancy in the participating minerals does not allow us to decipher which mineral pairs govern the evolution of the Hongjesa granite. However, the observed trends of trace elements in Fig. 8b and e do not define a relatively flat slope or a significant change in the Rb concentration indicative of partial melting process.

The above modelling is only an approximation, because the composition of primitive magma, the proportion of fractionating minerals, and the change of distribution coefficients during fractionation are unknown. However, we conclude from the available data including major and trace element chemistries and mineral compositions that the fractional crystallization has played an important role for the evolution of the Hongjesa granite.

AFM modelling of the Hongjesa granite

The magmatic evolution from biotite granite to biotite-muscovite granite in the Hongjesa pluton can be accounted for by using the AFM diagram. Fig. 9 shows mineral and bulk rock compositions of the Hongjesa granite in conjunction with the AFM liquidus topology (Abbott, 1981, 1985; Zen, 1988). The bulk composition of biotite granite lies in the less aluminous and more ferromagnesian

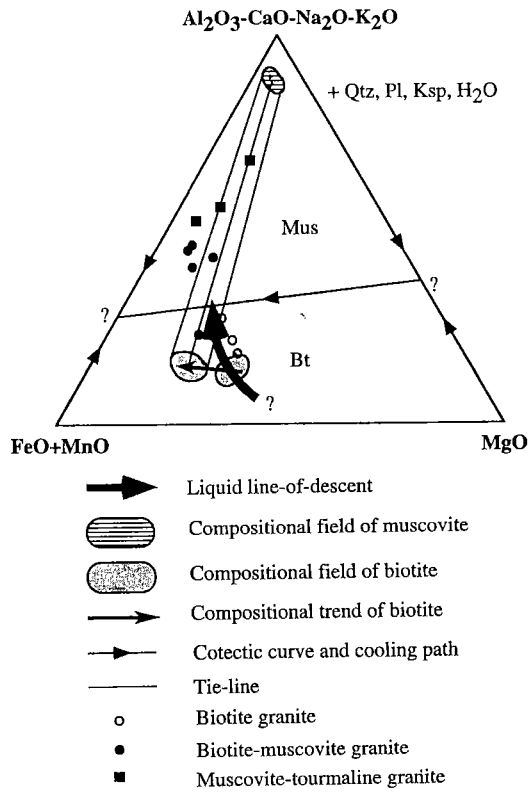

Fig. 9. Liquidus topology in the system (Al_2O_3-CaO-Na_2O-K_2O)-(FeO+MnO)-MgO (adopted from Abbott, 1981, 1985). The analyzed bulk compositions of biotite granite, biotite-muscovite granite, and muscovite-tourmaline granite are also shown.

field than that of biotite-muscovite granite.

Relatively Mg-rich biotite initially crystallizes by the reaction of the type, liquid → biotite, from a primitive granitic magma of the unknown composition. Crystallization of biotite produces biotite granite and shifts the melt composition toward the biotite-muscovite cotectic curve along the path schematically shown in Fig. 9. Once encountering the cotectic curve, the melt crystallizes muscovite as well as biotite, forming the biotite-muscovite granite. Biotite crystallized at this stage is more ferrous than that of biotite granite.

Most of the Hongjesa granitic melts may solidify along the biotite-muscovite cotectic curve. However, more evolved granites such as garnet-bearing biotite-muscovite granite and muscovite-

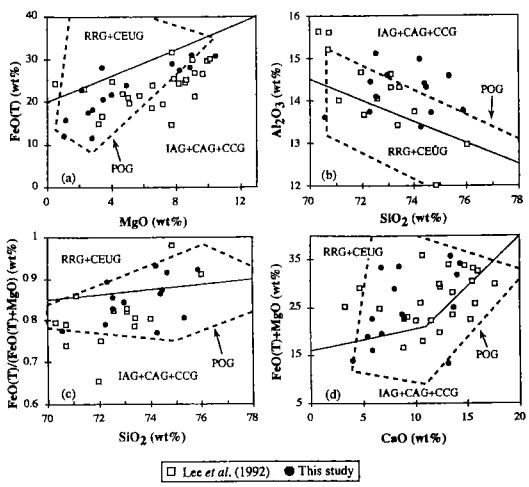

Fig. 10. Tectonic discrimination diagram (Maniar and Piccoli, 1989) using the major element data of the Hongjesa granite (Lee *et al.*, 1992; this study). Abbreviations: RRG, rift related granite; CEUG, continental epeirogenic uplift granite; POG, post-orogenic granite; IAG, island arc granite; CAG, continental arc granite; and CCG, continental collision granite.

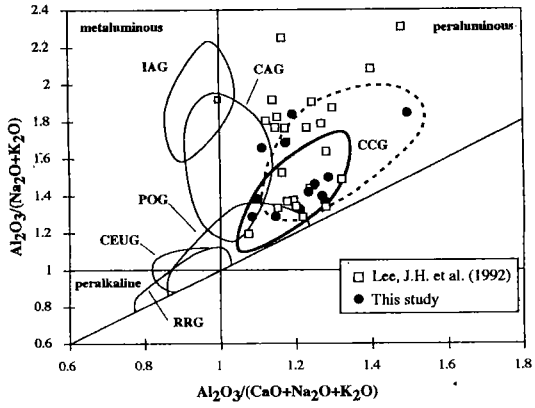

Fig. 11. $Al_2O_3/(CaO+Na_2O+K_2O)$ *vs.* $Al_2O_3/(Na_2O+K_2O)$ diagram of the Hongjesa granite. Each compositional field is from Maniar and Piccoli (1989). Thick curve represents the field of continental collision granite (CCG) of Maniar and Piccoli (1989). Dashed curve represents the compositional field of the CCG in Archean peraluminous granite (Breaks and Moore, 1992).

tourmaline granite uncommonly occur because of local enrichments in Mn and B, respectively. These incompatible elements are enriched in the melt by fractionation, and stabilize garnet and tourmaline as primary phase in late magmatic stage.

Tectonic setting and emplacement mechanism

Maniar and Piccoli (1989) have proposed the tectonic discrimination diagram of Phanerozoic granitoids using major oxides. On their plots of total FeO against MgO and Al_2O_3 against SiO_2 (Fig. 10a and b), the majority of the whole rock data for the Hongjesa granite belong to the field of orogenic granite. However, on other plots of Fig. 10c and d, compositional data do not define any specific field. Such a deviation may be attributed to the difference between tectonic processes in Phanerozoic and Proterozoic (Condie, 1989). In addition, the composition of granite may be influenced by not only tectonic processes but also source material, temperature and pressure (Roberts and Clemens, 1993).

In the $Al_2O_3/(CaO+Na_2O+K_2O)$ *vs.* $Al_2O_3/(Na_2O+K_2O)$ plot (Fig. 11), the Hongjesa granite primarily belongs to the continental collision granite (CCG) of Maniar and Piccoli (1989), but some of data are hardly accounted for by their discrimination diagram. Similar result is found in the late Archean peraluminous granite of the Superior Province, NW Ontario, Canada (Breaks and Moore, 1992). Most of our data, however, are compatible with the CCG field suggested by Breaks and Moore (1992). Hence, it is apparent from Figs. 10 and 11 that the Hongjesa granite has been associated with continental collision, as suggested from the trace element data by Hong (1992).

The spatial distribution of biotite granite in central part and biotite-muscovite granite in marginal part is unique for the Hongjesa granite, but difficult to explain. Zoning pattern in granitoid commonly changes from felsic to mafic granites towards the margin because of early crystallization near the pluton margin (Troll and Weiss, 1991; Gastil *et al.*, 1991). The reverse zoning may exceptionally occur by other mechanisms such as emplacement along the active thrust zone and assimilation with the wall rock (Leake, 1974;

Karlstrom *et al.*, 1993).

Patterns of foliation in the country rock are not systematically affected by the emplacement of the Hongjesa granite. In addition, the internal foliation of granite is not intensified towards the margin. The absence of micro- and macro-structures related to magmatic deformation suggests that the Hongjesa granite is emplaced by neither forceful intrusion such as ballooning or doming, nor deformation-related mechanism (Karlstrom *et al.*, 1993; Pitcher, 1993). Thus, we suggest that the biotite-muscovite granite is produced by passive stoping at the margin of the Hongjesa granite (Leake, 1974; Clarke, 1992). As fractionation proceeds, the country rocks are plucked into magma and exchange places with yet non-solidified, residual melt to form biotite-muscovite granite. The passive stoping accounts for not only the lack of contact aureole in the country rock but also the occurrence of partially melted xenoliths in granite.

CONCLUSIONS

The petrogenesis of the Hongjesa granite in the northeastern Sobaeksan Massif has been delineated on the basis of mineralogy and major element geochemistry. Primary conclusions of this study are summarized below.

1. The Hongjesa granitic pluton varies from biotite granite in the central part to biotite-muscovite granite in the marginal part. Muscovite-tourmaline granite sporadically occurs in the central part, while migmatitic granite enriched in biotite locally develops at the margin of pluton.

2. The X_{Fe} and ASI values of biotite increase from the center towards the margin of the pluton. The variations of mineral assemblage and chemistry are largely accounted for by the fractionation of granitic melt.

3. Biotite crystallizes as the primary ferromagnesian mineral at early magmatic stage, and the Al and Fe contents of melt consequently increase. As fractionation proceeds, muscovite co-crystallizes with biotite along the cotectic curve in the AFM diagram. Biotite of biotite-muscovite granite is enriched in the Fe content than that of biotite granite. Local enrichments of Mn and B may result in the subsequent crystallization of garnet and tourmaline, respectively.

4. The tectonic discrimination diagram using major element chemistry (Maniar and Piccoli, 19 89; Breaks and Moore, 1992) suggests that the Hongjesa granite may be associated with the continental collision. In addition, the peculiar zoning from biotite granite to biotite-muscovite granite towards the margin of the pluton is attributed to the passive stoping.

ACKNOWLEDGMENTS

This paper constitutes one chapter of an M.Sc. thesis of the senior author at Seoul National University and was supported by the Basic Science Research Institute Program, Ministry of Education, 1992, Project No. BSRI-92-504. Helpful and constructive reviews by Y.J. Kim, S.-T. Kwon and B. Ree are greatly appreciated.

REFERENCES

Abbott, R.N., Jr., 1981, The role of manganese in the paragenesis of magmatic garnet: An example from the Old Woman-Piute Range, California: A discussion. Jour. Geol., 89, 767-769.

Abbott, R.N., Jr., 1985, Muscovite-bearing granites in the AFM liquidus projection. Canadian Mineral., 23, 553-561.

Abbott, R.N., Jr. and Clarke, D.B., 1979, Hypothetical liquidus relationships in the subsystem Al_2O_3-FeO-MgO projected from quartz, alkali feldspar and plagioclase for $a(H_2O)<1$. Canadian Mineral., 17, 549-560.

Allan, B.D. and Clarke, B.D., 1981, Occurrence and origin of garnets in the South Mountain Batholith, Nova Scotia. Canadian Mineral., 19, 19-24.

Ayuso, R.A. and Arth, J.G., 1992, The Northeast Kingdom batholith, Vermont; magmatic evolution and geochemical constraints on the origin of Acadian granitic rocks. Contrib. Mineral. Petrol., 111, 1-23.

Benard, F., Moutou, P. and Pichavant, M., 1984, Phase relations of leucogranites and the significance of tourmaline in silicic magma. Jour. Geol., 93, 271-291.

Breaks, F.W. and Moore, J.M., Jr., 1992, The Ghost Lake batholith, Superior province of northeastern Ontario; a fertile, S-type, peraluminous granite-

rare-element pegmatite system. Canadian Mineral., 30, 835-875.

Brown, M., Friend, C.R.L., McGregor, V.R. and Perkins, W.T., 1981, The late Archean Qorqut granite complex of southern west Greenland. Jour. Geophys. Res., 86, B11, 10617-10632.

Chang, H.W., Lee, M.S. and Lee, J.M., 1988, The origin of geochemical variations in the Hongjesa granite gneiss. Jour. Geol. Soc. Korea, 24, 500-510.

Choo, S.H. and Lee, D.J., 1980, A Rb-Sr age determination on Precambrian granite in the Korean peninsula. KIER.

Clarke, D., 1992, NEWPET (computer software), Dept. of Earth Sci., Univ. of Newfoundland.

Clarke, D.B., 1992, Granitoid rocks. Chapman and Hall, London, 238p.

Condie, K.C., 1989, Plate tectonics and crustal evolution, 3rd ed., Pergamon, Oxford, 476p.

Gastil, G., Nozawa, T. and Tainosho, Y., 1991, The tectonic implications of asymmetrically zoned plutons. Earth Planet. Sci. Lett., 102, 302-309.

Guidotti, C.V., 1984, Micas in metamorphic rocks. In Micas (ed. P.H. Bailey), Rev. in Mineral., Mineral. Soc. Am., 13, 357-456.

Hanson, G.N., 1978, The application of the trace elements to the petrogenesis of igneous rocks of granitic composition. Earth Planet. Sci. Lett., 38, 26-43.

Holden, P., Halliday, A.M. and Stephens, W.E., 1987, Neodymium and strontium isotope content of microdiorite enclaves points to mantle input to granitoid introduction. Nature, 330, 53-56.

Holtz, F., Pichavant, M., Barbey, P. and Johannes, W., 1992, Effects of H_2O on liquidus phase relations in the haplogranitic systems at 2 and 5 kbar. Am. Mineral., 77, 1223-1241.

Hong, Y.K., 1985, Petrogenesis of the Proterozoic granitic rocks in the Buncheon-Seokpo area, NE Korea. Jour. Geol. Soc. Korea, 21, 196-209.

Hong, Y.K., 1992, Petrogenesis and evolution of early Proterozoic granitic rocks in the Northeastern Ryeongnam Massif, Korea. Jour. Geol. Soc. Korea, 28, 571-589.

Hong, Y.K. and Choi, T.Y., 1986, K-Ar ages on biotites of Proterozoic Buncheon and Hongjesa granitic rocks in the NE part of Sobaeksan Massif. Jour. Korean Inst. Mining Geol., 19, 147-151.

Ishihara, S., 1977, The magnetite-series and ilmenite-series granitic rocks. Mining Geol., 27, 293-305.

John, B.E. and Blundy, J.D., 1993, Emplacement-related deformation of granitoid magmas, southern Adamello Massif, Italy. Geol. Soc. Am. Bull., 105, 1517-1541.

Karlstrom, K.E., Miller, C.F., Kingsbury, J.A. and Wooden, J.L., 1993, Pluton emplacement along an active ductile thrust zone, Piute Mountains, Southeastern California: Interaction between deformational and solidification processes. Geol. Soc. Am. Bull., 105, 213-230.

Kim, H.S., Lee, S.M. and Lee, B.N., 1986, Petrogenesis of the Hongjesa granitic gneiss in the eastern part of Mt. Taebaeg area, Korea. Memoirs for Prof. Sang Man Lee's Sixtieth Birthday. University Text Publisher Co., Seoul, 107-133.

Kim, H.S., Lee, S.M., Kim, Y.K., Park, C.S., Kim, S.J. and Chang, H.W., 1991, Proterozoic magmatism and metamorphism in the northeastern part of Korea —Comparative studies between Buncheon and Pyeonghae granitic gneisses. Jour. Geol. Soc. Korea, 27, 614-625.

Kim, J., 1994, Petrogenetic study of the Hongjesa granite and the metasedimentary rocks in the northeastern Sobaeksan Massif. M.Sc. dissertation, Seoul National Univ.

Kim, J., Cho, M. and Kim, H.S., 1994, Metamorphism of the Hongjesa granite and the adjacent metasedimentary rocks (Magmatism and metamorphism of the Proterozoic in the northeastern part of Korea). Jour. Petrol. Soc. Korea (this issue).

Kim, J.H., *et al.*, 1989, A modelling study for the uranium exploration of the uraniferous Buncheon granites. Korea Electricity Co., 87M-T09, 540p.

Kim, T.K., 1991. Petrological and geochemical studies on the Buncheon granitic gneiss and its adjacent metasedimentary rocks in the northeastern part of the Sobaeksan Massif. Ph.D. dissertation, Seoul National Univ., 128p.

Kim, Y.J. and Lee, D.S., 1983, Geochronology and petrogenesis processes of the so-called Hongjesa granite in the Seokpo-Deogku area. Jour. Korean Inst. Mining Geol., 16, 163-221.

Kontak, D.J. and Corey, M., 1988, Metasomatic origin of spessartine-rich garnet in the South Mountain Batholith, Nova Scotia. Canadian Mineral., 26, 315-334.

Kresten, P., 1988, Granitization - fact or fiction? Geologiska Foreningens i Stockholm Forhandlingar, 110, 335-340.

Leake, B.E., 1974, The crystallization history and mechanism of emplacement of the western part of the Galway granite, Connemara, western Ireland. Mineral. Mag., 39, 498-513.

Lee, D.W., 1988, Lithogeochemical characteristics of granitoids in relation to tin mineralization in the Sangdong and Ulchin areas, Korea, and their applicability to tin exploration. Ph.D. dissertation, Seoul National Univ., 153p.

Lee, J.H., Won, J.K. and Park, S.I., 1992, The study of basement of metamorphic complex. In Geotectonical and petrographic studies: sedimentary, igneous and metamorphic rocks of Taebaek area, Kangwondo. KOSEF 88-1113-01, 402p.

Lee, K.J. and Cho, M., 1992, Metamorphism of the Gyeonggi Massif in the Gapyeong-Cheongpyeong area. Jour. Petrol. Soc. Korea, 1, 1-25.

Mahmood, A., 1983, Chemistry of biotites from a zoned pluton in Morocco. Mineral. Mag., 47, 365-369.

Maniar, P.D. and Piccoli, P.M., 1989, Tectonic discrimination of granitoids. Geol. Soc. Am. Bull.,

101, 635-643.
Manning, D.A.C. and Pichavant, M., 1988, Volatiles and their bearing on the behavior of metals in granitic systems. In Recent advances in the geology of granite related mineral deposits (eds. R.P. Taylor and B.F. Strong). Canadian Inst. Mining Metal., 39, 13-24.
McBirney, A.R., 1979, Effects of assimilation. In The evolution of the igneous rocks. Fiftieth anniversary respectives (ed. H.S. Yoder), Princeton Univ. Press, Princeton, 307-338.
McCarthy, T.S. and Hasty, R.A., 1976, Trace element distribution patterns and their relation to the crystallization of granitic melts. Geochim. Cosmochim. Acta, 40, 1351-1358.
Miller, G.F. and Stoddard, E.F., 1981, The role of manganese in the paragenesis of magmatic garnet: An example from the Old Woman-Piute Range, California. Jour. Geol., 89, 233-246.
Miller, G.F., Stoddard, E.F., Bradfish, L.J. and Dollase, W.A., 1981, Composition of plutonic muscovite: genetic implications. Canadian Mineral., 19, 25-34.
Montel, J.M., Didier, J. and Pichavant, M., 1991, Origin of surmicaceous enclaves in intrusive granites. In Enclaves and granite petrology (eds. J. Didier and B. Barbarin), Elsevier. Amsterdam, 509-528.
Na, K.C. and Lee, D.J., 1978, Petrological study of Hongjesa granite. Jour. Geol. Soc. Korea, 14, 103-112.
Park, K., Cheong, C., Lee, K. and Chang, H., 1993, Isotopic composition of lead in Precambrian granitic rocks of the Taebaeg area. Jour. Geol. Soc. Korea, 29, 387-395.
Paterson, S.R., Vernon, R.H. and Tobisch, O.T., 1989, A review of criteria for the identification of magmatic and tectonic foliations in granitoids. Jour. Struct. Geol., 11, 349-363.
Pitcher, W.S., 1993, The nature and origin of granite. Chapman and Hall, London, 321p.
Rhee, B.Y., 1991, Mineralogy of sericites in the Daehyeon Mine, Korea. Ph.D. dissertation, Seoul National Univ., 143p.
Roberts, M.P. and Clemens, J.D., 1993, Origin of high-potassium, calc-alkaline I-type granitoids. Geology, 21, 825-828.
Shand, S.J., 1951, The study of rocks. Thomas Murby and Co., London, 236p.
Shearer, C.K., Papike, J.L. and Laul, J.C., 1987, Mineralogic and chemical evolution of a rare-element granite-pegmatite system: Harney Peak Granite, Black Hills, South Dakota. Geochim. Cosmochim. Acta, 51, 473-486.
Speer, J.A., 1984, Micas in Igneous rocks. In Micas. (ed. P.H. Bailey), Rev. in Mineral., Mineral. Soc. Am., 13, 299-349.
Speer, J.A., 1987, Evolution of magmatic AFM mineral assemblages in granitoid rocks: the hornblende+melt=biotite reaction in the Liberty Hill pluton, South Carolina. Am. Mineral., 72, 863-878.
Speer, J.A. and Becker, S.W., 1992, Evolution of magmatic and subsolidus AFM mineral assemblages in granitoid rocks; biotite, muscovite, and garnet in the Cuffytown Creek Pluton, South Carolina. Am. Mineral., 77, 821-833.
Spry, A., 1969, Metamorphic textures. Pergamon, London, 650p.
Tindle, A.G. and Pearce, J.A., 1981, Petrogenetic modelling of in-situ fractional crystallization in the zoned Loch Doon pluton, Scotland. Contrib. Mineral. Petrol., 78, 196-207.
Tindle, A.G. and Pearce, J.A., 1983, Assimilation and partial melting of continental crust; evidence for the mineralogy and geochemistry of autoliths and xenoliths. Lithos, 16, 185-202.
Troll, G. and Weiss, S., 1991, Structure, petrology and emplacement of plutonic rocks. In Equilibrium and kinetics in contact metamorphism (ed. G. Voll), Springer, 39-66.
Yun, H.S., 1983, K/Ar ages of micas from Precambrian and Proterozoic rocks in the Northeastern part of Republic of Korea. Schweiz. Mineral. Petrograph. Mitt., 63, 295-300.
Yun, S.K., 1967, Geologic map of Jangseong sheet, Geol. Survey Korea, 25p.
Zen, E-An, 1986, Aluminum enrichment in silicate melts by fractional crystallization: Some mineralogic and petrographic constraints. Jour. Petrol., 27, 1095-1117.
Zen, E-An, 1988, Phase relations of peraluminous granitic rocks and their petrogenetic implications. Ann. Rev. Earth Planet. Sci., 16, 21-51.
Wall, V.J., Clemens, J.D. and Clarke, D.B., 1987, Models for granitoid evolution and source compositions. Jour. Geol., 95, 731-749.
Winkler, H.G.F., 1979, Petrogenesis of metamorphic rocks, 5th ed., Springer, New York, 348p.

(책임편집 : 권성택)

선캠브리아 홍제사 화강암의 진화과정
(한국 북동부지역의 원생대의 화성활동과 변성작용)

김정민 · 조문섭

서울대학교 자연과학대학 지질과학과

요 약: 선캠브리아 홍제사 화강암은 중앙부의 흑운모화강암으로부터 주변부로 갈수록 흑운모-백운모 화강암으로 변한다. 흑운모의 X_{Fe} (=Fe/(Fe+Mg)) 값과 알루미늄 포화도는 광물조합에 따라 체계적으로 변화하고 전암의 화학조성과 정의 상관관계를 보인다. 이러한 변화는 화강암체내의 누대구조와 함께 홍제사 화강암질 마그마의 분별정출작용에 기인한다. 미량원소 자료 또한 흑운모-백운모 화강암이 흑운모 화강암에 비해 더 진화하였음을 지지한다. 홍제사 화강암의 진화는 AFM 액상도 ($A=Al_2O_3-CaO-Na_2O-K_2O$; $F=FeO+MnO$; $M=MgO$)를 사용하여 잘 설명된다. 흑운모만 정출하는 초기 마그마단계에서 화강암질 마그마의 X_{Fe} 값과 알루미늄 포화도는 동시에 증가한다. 이후에 백운모가 흑운모-백운모 공융선을 따라 흑운모와 함께 정출하며, 그 결과 흑운모-백운모 화강암이 산출된다. 국부적으로 Mn과 B이 증가함에 따라 석류석과 전기석이 정출된다. 화강암체 주변부에서 흑운모-백운모 화강암이 산출하는 특징적 누대구조는 홍제사 화강암 관입시의 수동적 스토핑(passive stoping)에 의해 설명될 수 있다. 주성분 원소를 사용한 분별그림은 홍제사 화강암이 대륙 충돌 환경하에서 관입하였음을 지시한다.

핵심어 : 홍제사 화강암, 흑운모화강암, 흑운모-백운모 화강암, 분별정출작용, 액상도